Antisymmetrized, microscopic calculation for the $^{40}Ca(n,n)$ optical potential

F. Osterfeld and J. Wambach*
Institut für Kernphysik, Kernforschungsanlage Jülich, D-5170 Jülich, Federal Republic of Germany

V. A. Madsen
Institut für Kernphysik, Kernforschungsanlage Jülich, D-5170 Jülich, Federal Republic of Germany and Department of Physics, Oregon State University, Corvallis, Oregon 97331

(Received 15 July 1980)

An antisymmetrized second-order microscopic calculation of the imaginary optical potential for $^{40}Ca(n,n)$ is made using random-phase approximation transition densities to the intermediate excited states. An optical Green's function is used for the intermediate projectile propagator. Both inelastic and (n,p) charge exchange intermediate states of the nucleus are included and a finite range effective projectile-target nucleon interaction is used. The local approximation to the calculated imaginary optical potential is surface peaked but at a smaller radius than most of the phenomenological potentials, and the depth is somewhat smaller. Collectivity and intermediate charge-exchange states are shown to play an important role.

[NUCLEAR REACTIONS (n,n) scattering, calculation of optical potential; $E = 30$ MeV.]

I. INTRODUCTION

The microscopic calculation of the optical potential for elastic nucleon-nucleus scattering comprises one of the most challenging and most basic problems in nuclear physics. From the point of view of the many-body theory the optical potential has been identified with the mass or self-energy operator of the one-particle Green's function.[1] The mass operator is the so-called generalized optical potential which is nonlocal and complex and which depends on the incident energy E of the incoming nucleon. The mass operator automatically includes the exchange effects between the projectile and the nucleons in the target, and it allows for a diagrammatic expansion of the optical potential in terms of the $(A+1)$ many-body correlations. The optical potential, being an operator which allows the replacement of the $(A+1)$ many-body scattering problem by a one-body problem, cannot be calculated exactly since it would mean solving the many body problem itself. Therefore one always has to rely on certain approximations to the mass operator in real calculations.

Basically two different approaches have been formulated. One is the so-called "nuclear matter approach" of Jeukenne, Lejeune, and Mahaux[2,3] and Brieva and Rook[4] in which they consider the large target limit ($A \to \infty$, A = nucleon mass number) and calculate either the optical potential[2,3] or the two nucleon t matrix[4] in nuclear matter. They then obtain the optical potential for finite nuclei by making either a local density approximation on the potential itself[2,3] or on the two-nucleon t matrix,[4] which is then folded into the target ground state density distribution to get the optical potential. This approach has the advantage that it starts from a realistic nucleon-nucleon interaction and allows for a more or less parameter-free calculation of the optical potential in nuclear matter, but, on the other hand, it does not take into account any specific effects which are due to the finiteness of the nucleus, such as the possibility of collective shape oscillations, rearrangement collisions, etc.

Another approach is the so-called "nuclear structure approach" of Vinh Mau and Bouyssy[5,6] and Bernard and Van Giai[7] in which one assumes that the effective nucleon-nucleon interaction is basically known, but in which the inelastic excitations of the finite nucleus are taken into account. While the nuclear matter approach includes inelastic excitation effects of a finite nucleus only in an average way (via the local density approximation), the nuclear structure approach treats them explicitly and therefore includes specific features of the target nucleus in detail. The correct treatment of the energetically open reaction channels, however, should be especially important in determining the imaginary part of the optical potential, since the absorption should be quite sensitive to the nature and number of the energetically open intermediate channels. The authors of Ref. 5 performed a fully microscopic, antisymmetric calculation of the optical potential using a phenomenological effective interaction of δ-function type, the random-phase approximation (RPA) vectors of Gillet-Sanderson[8] for the intermediate target states, and a free-particle propagator for the intermediate projectile. Similar in approach are

the calculations in Ref. 7 where the RPA is solved in coordinate space and a Skyrme force has been used for the effective interaction.

Calculations of the optical potential have also been performed on a somewhat more phenomenological basis by Rao, Reeves, and Satchler[9] who start from Feshbach's formalism[10] and evaluate the optical potential in second order perturbation theory using collective form factors for the excitation of the intermediate states and an optical model propagator. Exchange effects are assumed to be implicitly included in the collective form factors. These authors have to postulate artificial open channels at low excitation energies in order to exhaust low multipole sum rules. Also Coulter and Satchler[11] have found that pickup-stripping (p-d-p) processes contribute appreciably to the absorption.

The purpose of this paper is to present a fully antisymmetric, microscopic calculation of the imaginary optical potential for ^{40}Ca(n,n) calculated to second (the leading) order in a finite-range projectile, target-nucleon interaction. The Eikemeier-Hackenbroich potential[12] is used for this interaction and the RPA wave functions of Krewald and Speth[13] are used for intermediate states. The calculations are similar in approach to those of Refs. 5–7 and to a large extent corroborate the results of the latter, calculated with similar approximations. The additional features of our calculations are the use of the optical instead of the free-particle Green's function for propagation of the intermediate projectile, the larger (up to $3\hbar\omega$) basis for the RPA wave functions, and the explicit inclusion of charge exchange intermediate states. All open RPA particle-hole states are included, so in leading order no nuclear states are neglected. We make the double-counting correction[5,6] which occurs due to the identity of the projectile and target nucleon in the leading order (noninteracting particle and hole) RPA graphs.

It is well known[5,6,9] that the imaginary optical potential is, in principle, nonlocal (see Sec. II). It will be shown in Sec. III that the nonlocality can be very large. We nevertheless follow the usual practice and take a local approximation using the formula of Perey and Saxon.[14] In Sec. II a brief review of the theory of the optical potential is given along with some illustrations of the double counting problem. Section III gives a discussion of the calculational ingredients and procedures used in obtaining the optical potential. Section IV presents some sample cases in order to illustrate the dependence of the calculations on assumptions or parameters of the theory. Also the principal result, the calculated optical potential for 30 MeV ^{40}Ca(n,n), is discussed. Section V contains a summary and conclusions.

II. THEORY

In second order the generalized imaginary optical potential for a *nonidentical* projectile is[9,10]

$$W(\vec{r},\vec{r}') = \mathrm{Im}\sum_N \langle 0|V|N\rangle_{\vec{r}}\, g_N(\vec{r},\vec{r}')\langle N|V|0\rangle_{\vec{r}'}\,, \tag{1}$$

where the matrix elements are over the nuclear coordinates only, and g_N is a projectile optical Green's function (see Sec. III) evaluated at an energy $E-E_N$, E_N being the excitation energy of the target nuclear state N. Obviously W is nonlocal. Because of the restriction to second order, only the intermediate particle-hole strength is directly excited. Since the RPA gives a good description of the particle-hole strength including collective effects, it is advantageous to use available RPA transition densities for the intermediate excitation.

Particle identity, however, introduces some essential complications, which have been treated by several authors[5-7] using the Green's function formalism, in which the optical potential is identified[1] with the mass or proper self-energy operator[15] $S^*(x,x')$. The operator S^* is the sum of all proper self-energy graphs connected to the projectile particle line.

By comparison with Eq. (1), Villars[16] gives the following expression for the exact optical potential $\mathcal{U}$ (in momentum space)

$$\mathcal{U} = U_{\mathrm{HF}}(k',k) + \sum_n S^{(n)}(k',k) \tag{2}$$

with

$$S^{(n)} = \sum_{p+s+r=n} \left\langle 0\left|\left(V\frac{1}{E_0-H_0}\right)^p J(k')\frac{1}{E-H_0+i\eta}\left(V\frac{1}{E-H_0+i\eta}\right)^r J^\dagger(k)\left(\frac{1}{E_0-H_0}V\right)^s\right|0\right\rangle_{\mathrm{LC}}$$
$$-\left\langle 0\left|\left(V\frac{1}{E_0-H_0}\right)^p J^\dagger(k)\left(\frac{-1}{E+H_0-i\eta}\right)\left(V\frac{-1}{E+H_0-i\eta}\right)^r J(k')\left(\frac{1}{E_0-H_0}V\right)^s\right|0\right\rangle_{\mathrm{LC}}, \tag{3}$$

where the subscript LC means linked cluster, E is the total energy, E_0 is the ground state energy of the target nucleus, $|0\rangle$ is the Hartree-Fock ground state, H_0 is the unperturbed Hartree-Fock Hamiltonian, and

$$J(k) = [a_k, V] = \sum_{\beta\gamma\delta} a_\beta^\dagger \langle k\beta|V|\gamma\delta\rangle a_\delta a_\gamma\,, \tag{4a}$$

$$J^{\dagger}(k)=[V,a_k^{\dagger}]=\sum_{\lambda\mu\nu}a_\lambda^{\dagger}a_\mu^{\dagger}\langle\lambda\mu|\,V\,|k\nu\rangle a_\nu\,. \tag{4b}$$

The diagrammatic perturbation expansion then includes only connected diagrams which cannot be separated into two parts by cutting only the projectile particle line. $J(k)$ is a potential for interaction of the projectile with the nucleus and therefore plays the role of the projectile, target-nucleon interaction in Eq. (1). The independent sum over s or p operating on the $|0\rangle$ with the LC restriction gives the exact target ground state wave function, and the independent sum over r gives for the operator between the $J^{\dagger}$ and J the exact Green's function, making the connection with Eq. (1) more apparent.

For nuclear scattering or in any case where the potential is strong or singular, the potential V may not be used directly in Eqs. (3) and (4). Rather one must take the antisymmetrical Schrödinger equation used by Villars as a starting point, apply a projection operator P onto a reasonably tractable model space with the complementary projection operator Q projecting onto states of very high energy and momenta of two particles. These two-body states are important both because they are excited by the strong short-range part of the two-body potential, and because they must be eliminated in the projection process in order to leave a reasonably well behaved effective interaction in the P space. Such an effective interaction need no longer be of two-body character, but will be approximately so if only two-body states were important in the eliminated Q space. From here on it will be assumed that such a projection has been possible and that the V remaining in Eqs. (3) and (4) is a well-behaved effective interaction, a t operator.

Equation (3) has been evaluated approximately by Vinh Mau by treating target nuclear states in RPA and allowing only second-order interactions with the projectile, which occupies independent-particle states. Although Eq. (3) is exact, when intermediate states of a product type like this are used there occurs a double counting[5,6] due to the identity of projectile and target nucleons. It is present, however, only in leading order diagrams, for which certain intermediate states of the $A+1$ system are counted twice when all intermediate states of both target and projectile are summed separately. It is essentially a nonorthogonality correction due to the fact that configurations consisting of a projectile particle and a target particle-hole state may not be orthogonal to the same sort of configuration when the particles are exchanged by antisymmetrization.

In the Appendix the imaginary part of Eq. (2) is evaluated to second order in the projectile, target-nucleon interaction, including the double counting correction. The target states are, in principle, treated to all orders of V, resulting in the following expression for W:

$$W(\vec{k}',\vec{k})=\mathrm{Im}\sum_{N,q>f}\Big[\langle\Psi_0|\,J(\vec{k}',\vec{q})\Psi_N\rangle\,\frac{1}{E-\epsilon_q-E_N+i\eta}\times\langle\Psi_N|J(\vec{q},\vec{k})|\Psi_0\rangle-\tfrac{1}{2}\langle\varphi_0|J(\vec{k}',\vec{q})|\varphi_N\rangle\times\frac{1}{E-\epsilon_q-E_N^{(0)}+i\eta}\langle\varphi_N|J(\vec{q},\vec{k})|\varphi_0\rangle\Big], \tag{5}$$

where

$$J(q,k)=\sum_{\beta\gamma}a_\beta^{\dagger}\langle q\beta|\,V\,|k\gamma\rangle a_\gamma \tag{6}$$

is a Hermitian one-body operator representing the effect of the scattering of the projectile, including exchange, on the target nucleus. In Eq. (5) Ψ_0 and Ψ_N denote the exact ground state and the exact excited states of the A-nucleon system, respectively, while φ_0 and φ_N denote the corresponding states of the *uncorrelated* system.

It is, of course, inconsistent to treat target nucleons and projectile nucleons differently. We have simply considered the interaction with the projectile in the lowest order in which an imaginary potential appears. Some justification for the inconsistency can perhaps be given by the following considerations. It is known from coupled-channel calculations that at very low projectile energies the effects of multistep processes are very large, while at higher energies although perhaps not negligible, they are much less important. One can in many cases calculate reliably with distorted-wave Born approximation (DWBA), and where DWBA is not good enough the multiple scattering nevertheless converges quite rapidly. Thus at several tens of MeV we expect that the lowest order in the projectile, target-nucleon interaction gives meaningful results.

III. DETAILS OF CALCULATION

A. Optical potential

In Eq. (5) the function

$$\langle\Psi_N|\,J(q,k)\,|\Psi_0\rangle=\Big\langle qN\Big|\sum_i V_{0i}(1-\rho_{0i})\Big|k0\Big\rangle\equiv\langle q|\,F_{N0}\,|k\rangle\,, \tag{7}$$

where F_{N0} is an antisymmetrized first-order nuclear matrix element for the excitation of state N from the ground state. It contains the exchange operator, which operates on the projectile wave

function of Eq. (5) exchanging the target-particle index with that of the projectile. It is calculated according to the formulation of Wambach *et al.*[17,18] using the nonlocal form for the antisymmetrized interaction $V_{0i}(1-P_{0i})$:

$$F_{N0}=F^D_{N0}+F^E_{N0}, \tag{8a}$$

$$F^D_{N0}=\delta^3(\vec{r}_0-\vec{r}_0')\left\langle N\left|\sum_i V(\vec{r}_0-\vec{r}_i)\right|0\right\rangle, \tag{8b}$$

$$F^E_{N0}=\left\langle N\left|\sum_i \delta(\vec{r}_0-\vec{r}_i')\delta(\vec{r}_0'-\vec{r}_i)v(\vec{r}_0-\vec{r}_i)\right|0\right\rangle, \tag{8c}$$

where D and E stand for direct and exchange, respectively, and where

$$v(0,i)\equiv V(0,i)P_\sigma(0,i)P_\tau(0,i) \tag{9}$$

is simply a two-body potential with an exchange mixture generally different from that of $V(0,i)$.

Equation (5) may then be written in r-space representation as

$$W(\vec{r}_0,\vec{r}_0')=\mathrm{Im}\Big[\sum_N\int\int F^*_{N0}(\vec{r}_0,\vec{r}_0'')\,g_N(\vec{r}_0'',\vec{r}_0''')\times F_{N0}(\vec{r}_0''',r_0')d^3r_0''d^3r_0''' -\tfrac{1}{2}\text{like sum for particle-hole states}\Big]. \tag{10}$$

The spin and angular integrals can be evaluated in closed form, leaving the $dr_0''dr_0'''$ radial integrals to be evaluated numerically with a computer. The final form of $W(\vec{r}_0,\vec{r}_0')$ is given by

$$W(\vec{r}_0,\vec{r}_0')=\mathrm{Im}\Big[\sum(-1)^{J_A-M_A}(\tfrac{1}{2}m_a\tfrac{1}{2}-m_b|s-\mathfrak{M}_s)(-1)^{1/2-m_b+s-\mathfrak{M}_s}(\mathcal{J}\mathfrak{M}_\mathcal{J}s\mathfrak{M}_s|\mathcal{L}-\mathfrak{M}_\mathcal{L}) \times(J_AM_AJ_A-M_B|\mathcal{J}\mathfrak{M}_\mathcal{J})(-1)^{\mathcal{L}-\mathfrak{M}_\mathcal{L}}\sum_{l_al_b}|i^{l_a}Y_{l_a}(\hat{r}_0)i^{l_b}Y_{l_b}(\hat{r}_0')|_{\mathcal{L}-\mathfrak{M}_\mathcal{L}}\sum_{J_N}\mathcal{F}^{l_al_bJ_N}_{\mathcal{L}s\mathcal{J}}(r_0,r_0')\Big] \tag{11}$$

with the nonlocal radial form factor

$$\begin{aligned}\mathcal{F}^{l_al_bJ_N}_{\mathcal{L}s\mathcal{J}}(r_0,r_0')=i^{l_a+l_b}\hat{\mathcal{J}}\hat{\mathcal{S}}\sum_{\substack{S_1L_1J_1S_2L_2J_2\\ l_cs_cj_c,\bar{S}_1\bar{S}_2}}&(-)^{J_N}W(J_AJ_1J_AJ_2,J_N\mathcal{J})(-)^{j_c-\bar{S}_2}B(l_al_cs_cj_c,L_1S_1J_1,\bar{S}_1)\\ &\times B(l_bl_cs_cj_c,L_2S_2J_2,\bar{S}_2)\,W(l_a\bar{S}_1l_b\bar{S}_2;j_c\mathcal{L})\begin{Bmatrix}J_2&s_c&\bar{S}_2\\J_1&s_c&\bar{S}_1\\\mathcal{J}&s&\mathcal{L}\end{Bmatrix}\\ &\times\int dr_0''r_0''^2\int dr_0'''r_0'''^2\left[\frac{\delta(r_0'-r_0''')}{r_0'r_0'''}(l_b0l_c0|L_20)F^D_{J_NJ_A,L_2S_2J_2}(r_0''')\right.\\ &\qquad\left.-F^E_{J_NJ_A,L_2S_2J_2,l_bl_c}(r_0',r_0''')\right]\\ &\times g_{l_cj_c}(r_0''',r_0'')\left[\frac{\delta(r_0-r_0'')}{r_0r_0''}(l_a0l_c0|L_10)F^D_{J_NJ_A,L_1S_1J_1}(r_0'')\right.\\ &\qquad\left.-F^E_{J_NJ_A,L_1S_1J_1,l_al_c}(r_0,r_0'')\right],\end{aligned} \tag{12}$$

where

$$B(l_al_cs_cj_c,L_1S_1J_1,\bar{S}_1)=(-)^{J_1}\frac{1}{\sqrt{4\pi}}\hat{l}_a\hat{l}_c\hat{s}_c\hat{j}_c\hat{L}_1\hat{S}_1\hat{\bar{S}}_1{}^2W(l_a\bar{S}_1l_cs_c;j_cL_1)W(J_1S_1\bar{S}_1s_c,L_1s_c) \tag{13}$$

and $\hat{j}=(2j+1)^{1/2}$. The quantity $g_{l_cj_c}(r_0''',r_0'')$ in Eq. (12) is the radial part of the optical Green's function describing the propagation of the intermediate projectile, and the quantities F^D and F^E are defined by

$$F^D_{J_NJ_A,LSJ}(r_0)=\sum_{n,\lambda}(-)^{L+\lambda}\hat{n}\hat{J}W(L\lambda SS,nJ)\int dr\,r^2\rho^{J_NJ_A}_{\lambda SJ}(r)v^n_{L\lambda}(r_0,r) \tag{14a}$$

and

$$\begin{aligned}F^E_{J_NJ_ALSJl_al_c}(r_0,r_0'')=(-)^{L+l_a}\frac{1}{\sqrt{4\pi}}\hat{L}\hat{J}^2\sum_{\substack{a,a_2n\\l_1l_2\lambda}}&(-)^{l_1+\lambda}\hat{a}_1\hat{a}_2\hat{\lambda}^2W(L\lambda SS,nJ)(l_c0a_20|l_10)(l_a0a_10|l_20)\\ &\times\begin{Bmatrix}a_1&a_2&n\\l_a&l_c&L\\l_2&l_1&\lambda\end{Bmatrix}\rho^{J_NJ_A}_{l_1l_2\lambda SJ}(r_0,r_0'')v^n_{a_1a_2}(r_0,r_0''),\end{aligned} \tag{14b}$$

respectively. In Eqs. (14) the coefficients $v^n_{a_1a_2}$ arise from the multipole expansion[19] of the central ($n=0$) and tensor ($n=2$) parts of the effective direct (V) and exchange (v) two nucleon interactions, and the local and nonlocal nuclear transition densities are defined by

$$\rho^{J_N,J_A}_{\lambda SJ}(r_0)=\sum_{\substack{n_1l_1j_1\\ n_2l_2j_2}}(X^{J_N,J_A}_{j_1j_2}+Y^{J_N,J_A}_{j_1j_2})\frac{1}{\sqrt{4\pi}}\frac{\hat{1}}{2}\hat{S}\hat{j}_1\hat{j}_2\hat{J}\hat{\lambda}\hat{l}_1(l_1 0\lambda 0|l_2 0)\begin{Bmatrix} l_2 & \frac{1}{2} & j_2\\ l_1 & \frac{1}{2} & j_1\\ \lambda & S & J\end{Bmatrix} R_{n_2l_2j_2}(r_0)R_{n_1l_1j_1}(r_0) \tag{15a}$$

and

$$\rho^{J_N,J_A}_{l_1l_2\lambda SJ}(r_0,r_0')=\sum_{\substack{n_1j_1\\ n_2j_2}}(X^{J_N,J_A}_{j_1j_2}+Y^{J_N,J_A}_{j_1j_2})\frac{\hat{1}}{2}\hat{S}\hat{j}_1\hat{j}_2\hat{\lambda}\begin{Bmatrix} l_2 & \frac{1}{2} & j_2\\ l_1 & \frac{1}{2} & j_1\\ \lambda & S & J\end{Bmatrix} R_{n_2l_2j_2}(r_0)R_{n_1l_1j_1}(r_0'), \tag{15b}$$

where the $X_{j_1j_2}$ and $Y_{j_1j_2}$ are the RPA particle-hole amplitudes[20] and the $R_{n_il_ij_i}$ denote the radial single-particle wave functions.

Note that we have two terms in Eq. (11), namely one with $\mathcal{J}=0$, $\mathcal{L}=0$, $\mathcal{S}=0$, and the other with $\mathcal{J}=0$, $\mathcal{L}=1$, $\mathcal{S}=1$. Here only the $\mathcal{J}=\mathcal{L}=\mathcal{S}=0$ term is calculated, the $\mathcal{J}=0$, $\mathcal{L}=1$, $\mathcal{S}=1$ term corresponds to a nonlocal spin-orbit potential.

A program has been written to evaluate the imaginary part of the nonlocal optical potential of Eq. (11) given in detailed form in Eqs. (12)–(15). The calculation of the nonlocal form factor in Eq. (12) is a nontrivial problem since it involves for EE a 6-dimensional integration over a 12-dimensional function. Four integrations are in angle, which can be done in closed form, and two are in r space, which have to be performed numerically. For this reason one has to be very careful in choosing the right methods for the evaluation of Eq. (12). In our problem we make extensive use of the fact that the nonlocal form factors $F^E(r_0,r_0')$ are rather slowly varying functions of r_0 and r_0'. Therefore it has to be calculated at points of rather large stepsize (of typically 0.4 or even 0.8 fm) and the intermediate points are obtained by using spline-function interpolation methods. The form factors are interpolated onto the mesh of the Green's function which is oscillatory and which therefore is calculated on a small mesh (0.1 fm).

Note that the DD, DE, and ED terms in Eq. (12) involve either no integration or a single integral. Otherwise the calculation is the same as described above. Finally we want to mention that by using these interpolation methods the time for the calculation of the form factor in Eq. (12) can be shortened enormously, so the calculation of the contribution to the absorption of one intermediate state, described by a $3\hbar\omega$ RPA wave function, takes less than 30 sec on the IBM 3033.

B. Nuclear RPA wave functions

The RPA vectors obtained by Speth and Krewald[13] were used for the description of the intermediate nuclear states. In Ref. 13 the ph-residual interaction strength was chosen to match the energy and transition rate for the 3^- collective state as well as possible and to obtain the giant dipole and giant quadrupole resonances approximately at the right energies. The spurious 1^-, $T=0$ state was brought nearly to zero excitation energy and has not been included in the calculation of the optical potential. The 1^- strength agrees with the dipole sum rule and the 2^+ giant resonance strength at 18 MeV seen in (α,α') and (e,e') is reproduced. The basis consists of all shell model states from $0s_{1/2}$ to $5h_{11/2}$, including all $1\hbar\omega$, $2\hbar\omega$, and most $3\hbar\omega$ strengths.

Since only energetically open channels can contribute to the imaginary potential, all RPA intermediate states are summed up to the energy of the projectile, 141 states in all for 30 MeV neutron scattering. In the case of the 3^- state, the low-lying collective state has most of the strength (40% of the energy weighted sum rule), but for other multipolarities the strength is distributed over many states.

In order to show the relative contribution of different multipolarities λ^τ to the imaginary potential, the value of $W(r,r)$ is shown in Table I for $r=3.6$ fm, where the peak occurs. Since the nonlocality length of $W(r,r')$ does not vary greatly from one λ^τ to another, $W(r,r)$ gives a good account of the relative contribution to the equivalent local potential $\tilde{W}(r)$. As expected and as is seen in the table, the 3^- multipoles have the largest effect but 2^+, 4^+, and 5^- states also make essential contributions. Table I also gives for the 2^+ and 3^- multipolarities the contribution of pure particle-hole

TABLE I. Contribution of various multipoles to the diagonal nonlocal imaginary optical potential at the peak position.

λ^π	$W(3.6, 3.6)$ MeV fm^{-3}
0^+	−0.009
1^-	−0.067
2^+	−0.329
3^-	−0.503
4^+	−0.170
5^-	−0.112
6^+	−0.041
2^+ ph [a]	−0.07
3^- ph [a]	−0.142
3^- [b]	−0.329

[a] Pure particle-hole states.
[b] Lowest lying 3^- state only.

states to the optical potential. Although not negligible, they are rather small compared to the corresponding RPA transitions. The ground state correlations and the collectivity push strength to lower energies and increase greatly the absorption into states lower than the 30 MeV projectile energy. A comparison of the contributions to RPA and ph states to the local potential is given in Sec. IV.

C. Nonlocality and local approximation

The characteristics of the nonlocality are predominantly a result of the single particle projectile Green's function. For a free particle it has the form

$$\mathrm{Im}\, g_l^{(0)}(\vec{r},\vec{r}') = -\frac{2mk}{\hbar^2}\,\frac{\sin ks}{ks}\,, \tag{16}$$

where s is the nonlocality coordinate

$$s = |\vec{r} - \vec{r}'|\,. \tag{17}$$

Equation (16) has a characteristic structure with a large central peak and small positive and negative oscillations at large values of s. The nonlocality length b is defined as the value of s for which the function in question drops to e^{-1} of the value at $s=0$. For Eq. (16) $b \simeq 2.20/k$ fm. Thus one would expect the local approximation to be best at higher energies and the nonlocality length to be larger outside the nucleus, where the wave number is smaller. For 30 MeV neutrons we can expect a nonlocality length of $2.20/1.36 \simeq 1.6$ fm. This is a good rough estimate, as described below.

Although the optical Green's function (OGF)

$$\mathrm{Im}\, g(\vec{r},\vec{r}') = -\frac{2mk}{\hbar^2}\,\mathrm{Re}\sum_l R_l(r_<)R_l^{(+)}(r_>) \times \sum_m Y_{lm}(\hat{r})Y_{lm}^*(\hat{r}') \tag{18}$$

with

$$R_l^{(+)}(r) \to h_l^{(1)}(kr) \tag{19}$$

is much more complicated than (16) and depends on $R = (\vec{r}+\vec{r}')/2$ as well as on s, it retains the characteristic peaking at $r = r'$. The nonlocality, however, depends on the direction as well as on the magnitude of $\vec{s}$. The direct-direct contribution to the optical potential contains a summed product of Green's functions and form factors. The sum over intermediate states N of $\mathrm{Im}\, F_{0N} g_N F_{0N}^*$ sharpens the nonlocality (makes W more local than $\mathrm{Im}\, g_N$ alone). When exchange is included, these simple arguments do not apply unless the range of the two-body interaction is very small. However, the characteristic behavior of a peak at $r = r'$ and oscillation as a function of s still applies when all amplitudes DD, DE, ED, and EE are included. Inside the nucleus at small radii, the behavior of $W(r, r')$ is sometimes peculiar, the positive oscillations being rather large. In this region the local approximation does not make sense, so we have simply ignored it, knowing that this inner region is also not very important for the scattering.

The local approximation is made as in Ref. 5 neglecting cross-derivative terms in the formula of Ref. 14, generalized slightly to include different contributions to the $\vec{s}$ integral from different directions. For $\mathcal{L} = 0$, Eq. (11) is independent of the directions of $\vec{r}_0$ and $\vec{r}_0'$ for a given angle θ between the two vectors. Since, for spin transfer $S=0$, $W(\vec{r}_0, \vec{r}_0')$ is a spatial scalar, it cannot depend on the direction of the vector $\vec{R} = (\vec{r}_0 + \vec{r}_0')/2$. Thus W must depend on only three coordinates, $R = |\vec{R}|$, $|\vec{s}|$, and the angle between $\vec{R}$ and $\vec{s}$ (or alternatively r_0, r_0', θ). Since the radial form factor is symmetric in r_0 and r_0', W is also symmetric with respect to a reflection of $\vec{s}$ through the $\vec{s}_\perp \vec{R}$ plane. We therefore use a symmetric Gaussian form to approximate the nonlocality,

$$W(r_0, r_0') = W(R,R)\,\exp\{-[s_\parallel{}^2/b_\parallel{}^2(R) + s_\perp{}^2/b_\perp{}^2(R)]\}\,, \tag{20}$$

where $s_\parallel = s \cdot \hat{R}$ and $s_\perp = (s^2 - s_\parallel{}^2)^{1/2} \simeq R\theta$. This form neglects the difference between cord and arc, which can make differences of 5% for the largest nonlocality angles. Figure 1 shows the parallel and perpendicular width functions $b_\parallel$ and $b_\perp$ for W. The nonlocality increases steadily from small values of R within the nucleus to the largest values required. The perpendicular nonlocality is somewhat larger than the parallel nonlocality at larger radii. The nonlocality angle is more nearly constant than the $b_\perp$. The rough value of $b = 1.6$ fm from the free particle Green's function is seen to be relevant. The local approximation[14]

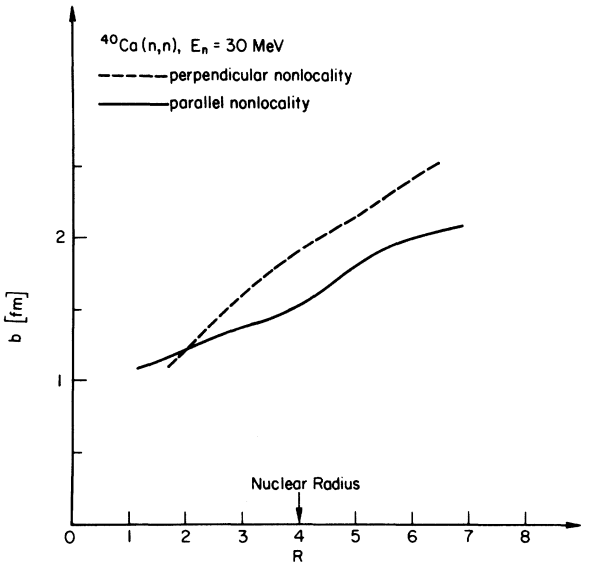

FIG. 1. The nonlocality length arising in the local approximation to the optical potential. The parallel nonlocality is in the radial coordinate for zero angle between $\vec{r}$ and $\vec{r}'$ and the perpendicular nonlocality is for $r=r'$ but nonzero angle. In each case b is the e^{-1} falloff distance.

is then made to Eq. (20) giving the equivalent local form

$$W(R)=W(R,R)\pi^{3/2}b_{\parallel}(R)b_{\perp}^{2}(R) \times\exp(-[b_{\parallel}^{2}(R)+2b_{\perp}^{2}(R)]\{2m[E-V(R)]/\hbar^{2}\}/12), \quad (21)$$

where $V(R)$ and E are the potential and total energy of the incident projectile.

IV. RESULTS AND DISCUSSIONS

A calculation of the imaginary part of the optical potential has been performed for the ^{40}Ca(n,n) reaction at an incident energy of 30 MeV. Before presenting the final results, however, we first describe some illustrative examples, where we have limited the intermediate states to be either the low-lying 3^- collective state or to be all the energetically open 3^- states.

We discuss these illustrative examples in order to describe important physical effects which are somewhat independent of the nature and number of intermediate states.

A. Some illustrative sample calculations

1. Effect of optical Green's function

As in the work of Satchler *et al.*[9] we have used an optical Green's function for the intermediate-projectile propagator. Neglecting spin-orbit and imaginary potentials, one may write the Green's function of Eq. (18) in an eigenfunction expansion

$$g_N^{(+)}(r,r')=\sum_{lmn}\frac{\Psi_{nlm}(r)\Psi_{nlm}^{*}(r')}{E-E_N-\epsilon_{nl}+i\epsilon}, \quad (22)$$

where Ψ_{nlm} is a single-particle eigenstate, E_N is the energy of the intermediate nuclear state, and ϵ_{nl} is the single-particle eigenenergy. The sum includes bound single-particle states as well as unbound ones. Because of exclusion of the projectile by nucleons in occupied states, a subtraction of these states should be made from g_N^{+} of Eq. (18). However, because for bound states the energy denominator can never be zero, the sum over any bound states is always purely real. (The numerator is also real.) Therefore, the exclusion of occupied bound states affects only the real and not the imaginary parts of the Green's function and optical potential.

When a real potential is used, this Green's function resonates sharply,[21] resulting in corresponding peaks in the optical potential. Because of absorption in the intermediate channel, not explicitly included in our calculation, there should be some imaginary part to the optical potential in which the intermediate projectile propagates. As in Ref. 7, as a matter of taste, we would prefer to use a Green's function for a real potential so all imaginary potentials which come out of the calculation are clearly a result of the theory and not of the parameters used. We therefore take the point of view that we use an energy-averaged intermediate Green's function consistent with the idea that optical potentials are energy-averaged quantities. Using the eigenfunction expansion form Eq. (22) and folding a Lorentzian of width Γ and E we get simply g evaluated at the complex energy $E+i\Gamma/2$. Inside the nucleus, the wave equation for this complex energy is identical to that with an absorptive optical potential $W=\Gamma/2$. Because our Green's function code can use only real energies and an absorptive optical potential, we use an absorptive potential of depth ~2 MeV to achieve qualitatively the same effect as in an energy averaged Green's function, to smooth out the intermediate single-particle resonances.

Figure 2 shows a comparison of the local-approximated optical potential $\tilde{W}$ for 9 MeV ^{40}Ca(n,n) scattering using only the low-lying 3^- state as an intermediate state calculated with both the optical Green's function (OGF) and free-particle Green's function (FPGF). The two results are very similar, which to a large extent gives justification for the use of FPGF in Ref. 5. The OGF is larger in the nuclear interior, particularly for the higher partial waves at this low energy. As a result the OGF tends to give a $\tilde{W}$ peaked at a slightly smaller

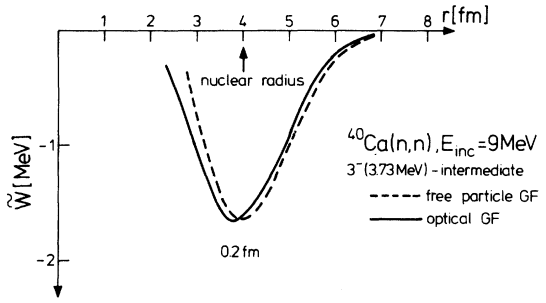

FIG. 2. The local equivalent potential $\tilde{W}(r)$ of the nonlocal optical potential $W(r, r')$ for neutrons of 9 MeV incident energy. The two curves, which compare $\tilde{W}(r)$ obtained with an optical Green's function to that using a free-particle Green's function, are calculated including absorption only from excitation of the first 3$^-$ state in ^{40}Ca.

radius than FPGF. Calculations were also made in which the imaginary part was increased to about one half the Becchetti-Greenlees value.[22] The resulting $\tilde{W}(R)$ was essentially identical to that used in Fig. 2 and in the rest of the calculations presented in this paper. It is remarkable how little the final result depends on how much the intermediate particle is absorbed. To the contrary, the use of plane waves in the initial or final projectile state of any direct reaction calculation would badly overestimate the scattering or reaction amplitude.

2. *Effect of exchange*

The effect and importance of exchange is shown by the comparison of Fig. 3. Because the Eikemeir-Hackenbroich interaction is spatially even, the exchange and direct contributions are constructive and, because there are three exchange contributions *ED*, *DE*, and *EE*, the effect of exchange is very large. It should be noted that the purely direct $\tilde{W}$ peaks at a slightly higher radius than the full potential. This effect is probably due to the fact that the nonlocal, one-step form factor for exchange contains a nuclear single-particle wave function factor not folded with the finite range potential. Both curves peak at points smaller than the nuclear radius, which is 4.00 fm in the Becchetti-Greenlees real potential.[22]

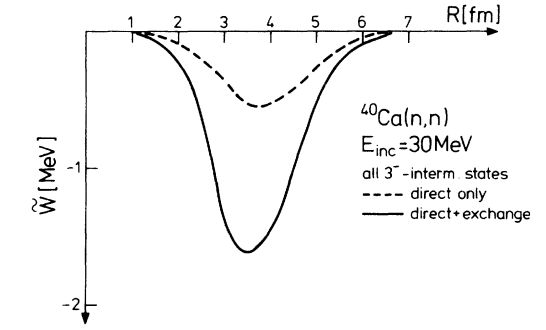

FIG. 3. A comparison of the locally approximated optical potential calculated with and without exchange contributions for 30 MeV incident energy neutrons with all open 3$^-$ states as intermediate states.

3. *Effect of density dependent forces*

Mahaux *et al.*[2,3] have calculated the imaginary optical potential in nuclear matter using the local density approximation to obtain the optical potential for finite nuclei. Any surface effects must then come from the local density approximation. The imaginary potential which they have obtained is peaked at the nuclear surface, due to the density dependence of the interaction. The results obtained here and in Refs. 5 and 6 also peak at the surface but at too small a radius. As a test of the effects of density dependence, we have used the singlet and triplet factors from Green's paper,[23] used there with the Kallio-Koltveit force, and multiplied them instead by the Eikemeier-Hackenbroich singlet and triplet central factors in order to get some idea of how much a reasonable density dependence can alter the peak position. Figure 4 shows that this particularly density dependence does increase W substantially in the region beyond the nuclear surface and shifts the peak position by about 0.4 fm to larger radii.

B. Full calculation of ^{40}Ca imaginary optical potential

1. *Contributions to the imaginary potential from different classes of intermediate states*

In the calculation of the imaginary part of the optical potential we include all energetically open intermediate states, i.e., all inelastically excited natural and unnatural parity states and also the corresponding natural and unnatural charge ex-

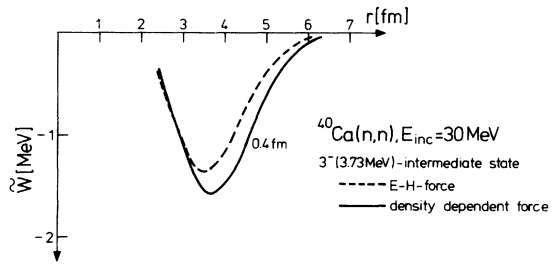

FIG. 4. The solid curve shows the effect on the locally approximated optical potential of including the singlet and triplet density-dependent factors of Green (Ref. 23) in the projectile, target-nucleon interaction.

change states. In a double closed shell nucleus such as ^{40}Ca most of the states in the low-excitation energy region are of natural parity, while the first unnatural parity states open up at higher excitation energies (~10 MeV). Therefore a large fraction of the absorption is due to the natural parity states, particularly the low-lying 3^- and 5^- states. At an incident energy of 30 MeV, however, the giant dipole, the isoscalar giant quadrupole, and also an appreciable fraction of the hexadecapole strength are excited and contribute substantially to the absorption. On the other hand, the unnatural parity states are less collective and therefore contribute less. In Fig. 5 we show the contributions to the imaginary potential which arise from the different classes of intermediate states. It is somewhat surprising that charge exchange gives such a large contribution to the absorption. This results from the fact that the charge exchange states in (n,p) reactions are shifted down in energy by the Coulomb energy differences of the nuclei (Z,N) and $(Z-1,N+1)$ and to the greater (×2) projectile matrix element for charge exchange compared to inelastic scattering. In Fig. 6 we show the total contributions of inelastic excitations and charge exchange reactions separately and find that charge exchange accounts for nearly 30% of the total absorption at the nuclear surface.

2. *Particle-hole corrections*

As has been already discussed in Sec. II we have to correct the RPA results for the contributions coming from the excitation of intermediate particle-hole doorway states, since otherwise we would count these contributions twice. Simultaneously this particle-hole doorway contribution is also the result which one would obtain with uncorrelated particle-hole intermediate states only. It can be seen from Fig. 7 that the particle-hole correction

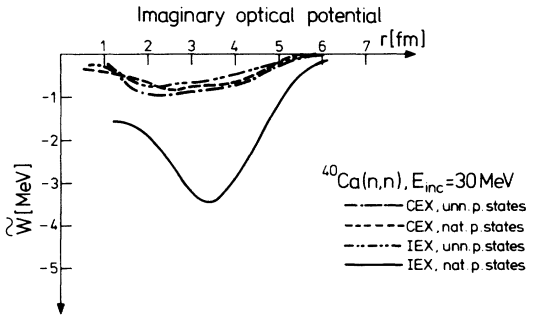

FIG. 5. Contributions to the imaginary optical potential from various types of intermediate states: unnatural and natural parity, charge exchange and inelastic scattering intermediate states.

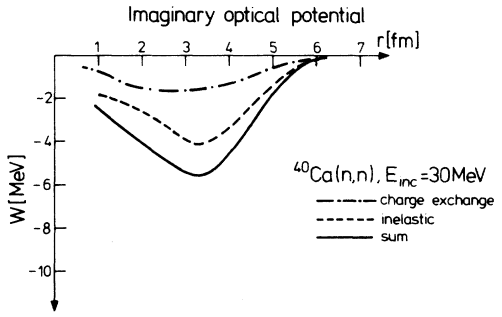

FIG. 6. Contribution to the imaginary optical potential from all charge exchange and all inelastic intermediate states.

is rather small. This means that a calculation with pure particle-hole intermediate states would greatly underestimate the absorption. Thus a large fraction of the absorption and surface peaked character must be attributed to the collective effects of a nucleus, which are reasonably well described by the RPA.

C. Comparison to other potentials

In Figs. 8 and 9 we compare our calculated potential with various phenomenological potentials and with the calculated potential of Vinh Mau.[6] Our imaginary potential is surface peaked, but the peak occurs at a smaller radius and is weaker than the phenomenological potentials by about 2 MeV. The underestimate in depth is perhaps not surprising since we include only the open inelastic channels explicitly but no rearrangement channels, which would make an added contribution to the absorption. A comparison between our calculation and that of Vinh Mau[6] shows that our potential peaks at a smaller radius and is also not as deep. Clarification of the difference between our

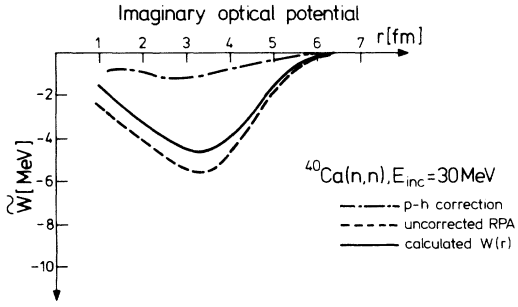

FIG. 7. Effect of the double counting (ph) correction to the imaginary optical potential. The dot-dashed curve is also the optical potential which is obtained for 30 MeV neutrons using all open particle-hole intermediate states. (It is itself already corrected for double counting.)

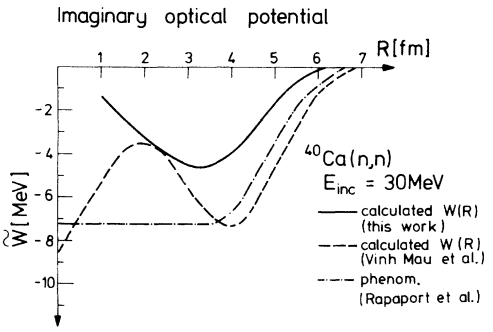

FIG. 8. Comparison of our optical potential with a similar calculation by Vinh Mau (Ref. 6) and a phenomenological potential (Ref. 24) at 30 MeV neutron energy.

result and that of Vinh Mau requires consideration of the following points.

(i) Our potential is calculated with an optical model Green's function, while that of Ref. 6 is obtained with a free propagator. An optical model propagator, however, shifts the peak of the potential by about 0.2 fm to the inner region of the nucleus (see Fig. 2).

(ii) We use the RPA-transition densities of Krewald and Speth,[13] while Vinh Mau uses those of Gillet and Sanderson.[8] A comparison of the RPA-transition densities for the low-lying 3^- collective state, for instance, shows that the Gillet-Sanderson transition density peaks at a larger radius (by about 0.3 fm) than that of Ref. 13.

(iii) The difference in depth, however, is harder to understand. The RPA calculations of Krewald and Speth have been performed in a model space which is appreciably larger (nearly all $3\hbar\omega$ excitations are included) than that in the calculations of Gillet and Sanderson. Therefore a larger fraction of the total transition strength especially for states of higher multipolarity is included, which should also lead to a more strongly absorbing potential. Moreover, charge exchange intermediate states, which are not considered in Vinh Mau's calculation, are included in our calculation of the optical potential and actually make a large contribution to the absorption. From these facts one would expect that our potential should be more strongly absorbing than that of Ref. 6. There is, however, an additional difference between the two calculations which concerns the effective projectile-target nucleon interaction used. In our calculations we use the Eikemeier-Hackenbroich force[12] which in average reproduces inelastic scattering cross sections for the low-lying collective states. This we have checked by performing microscopic, antisymmetrized DWBA calculations for these states using the RPA wave functions of Ref. 13. Therefore we may say that we have calibrated the effective projectile-target nucleon interaction to inelastic scattering before using it in the calculation of the optical potential. Vinh Mau, on the other hand, uses the Reichstein-Tang interaction[25] which gives inelastic cross sections which are larger by a factor of 1.5 than that obtained with the Eikemeier-Hackenbroich force. Therefore we would also obtain a 50% deeper imaginary optical potential if we used the Reichstein-Tang interaction. It would also, however, give too large an inelastic cross section. The effective projectile-target nucleon interaction is ambiguous and has to be calibrated somewhere, for instance from inelastic scattering, before it can be used in the calculation of the optical potential.

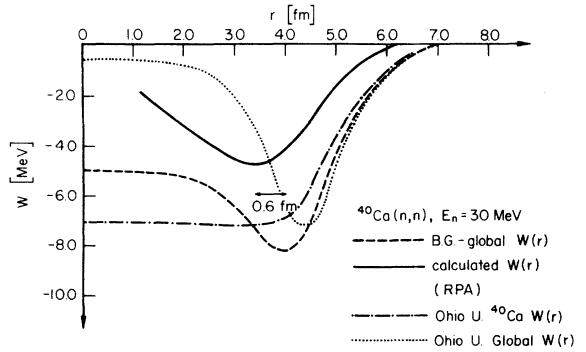

FIG. 9. Comparison of our calculated potential with phenomenological potentials of Becchetti-Greenlees (Ref. 22) and Ohio University (Ref. 24).

We have mentioned already that our calculated potential peaks somewhat below the nuclear radius, compared with most of the phenomenological potentials, like that of Refs. 22 and 24. As, however, has been discussed above already, a density-dependent effective projectile-target nucleon interaction has the tendency to shift the absorbing potential to larger nuclei. From this we may conclude that a density-dependent effective projectile target nucleon force together with the inclusion of nuclear collectivity will probably lead to a microscopic imaginary potential which has a surface form in agreement with phenomenological potentials. It is important to realize that the real microscopic potential is nonlocal and that we always compare the "equivalent local" potential with the phenomenological potentials. The nonlocality length in the surface region, however, is rather large, and the local approximation is therefore not very good.

D. Calculation of reaction cross sections

The imaginary part of the microscopically calculated, equivalent local potential has been used

in the calculation of the elastic scattering cross section for 30 MeV neutrons. We have simply replaced the imaginary part in the phenomenological potential of Ref. 24 with the microscopic one and obtain the result as shown in Fig. 10. The cross section calculated with the microscopic imaginary potential is larger than that obtained with the phenomenological one by roughly a factor of 2 at large angles. This overestimate is an indication for too little absorption, as expected from the results given in Figs. 8 and 9. Note that the reaction cross section of the microscopic potential, however, amounts to roughly 71% of the reaction cross section of the phenomenological potential. We have also calculated the total inelastic cross section to all natural parity, inelastic intermediate states by performing microscopic ADWBA calculations. The total inelastic scattering cross section to these states amounts approximately to 60 mb. Inclusion of charge exchange would probably increase this number by 50%, but we have not calculated it, since we wanted only a rough estimate of the total inelastic cross section.

Comparing the latter with the total reaction cross section shows that only ~10% of it is due to inelastic scattering. This demonstrates the effectiveness of inelastic channels as doorways to other reaction channels.

V. SUMMARY AND CONCLUSIONS

The calculation of the imaginary part of the nuclear optical potential W has been made to second order using a finite range effective projectile-target nucleon interaction and an optical Green's function for the intermediate-state propagation including exchange and all open inelastic and charge exchange RPA intermediate states. Besides the final calculation of W, the dependence on various parameters of the theory has been examined.

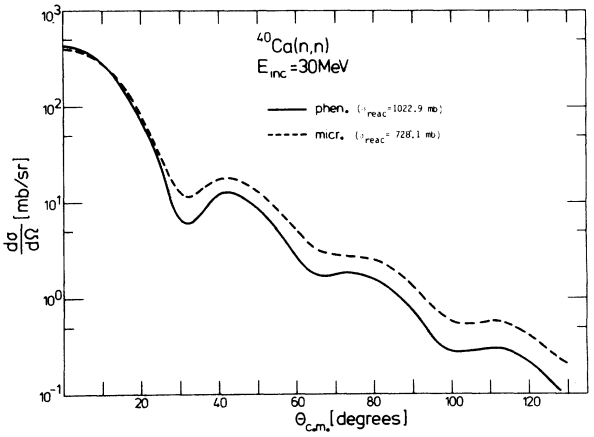

FIG. 10. Comparison of the differential cross section for 30 MeV ^{40}Ca(n,n) calculated using the phenomenological optical potential with that obtained replacing the imaginary part of the phenomenological potential by our microscopic potential.

The use of an optical Green's function instead of a free-particle Green's function makes a significant, though surprisingly small, difference in W, the main effect being a slight shift of the surface peak to smaller radii. Exchange is possible at each step of intermediate excitation and deexcitation and its effects on W is therefore multiplied compared, for example, to the effect on the real optical potential V, which results primarily from a one-step mechanism. For even forces, which we have used, the direct and exchange amplitudes are constructive, so inclusion of exchange increases W by a factor of more than 2. Charge exchange intermediate states are rather important, accounting for more than $\frac{1}{3}$ of W. The calculated W tends to be surface peaked due largely to surface-peaked transition densities of the important intermediate collective states. The position of the peak occurs at a somewhat lower radius than that of empirical optical potentials but a reasonable density dependence increases the radius of this peak. The collectivity of the dominant intermediate states is very important; a strongly surface-peaked optical potential does not occur when simple particle-hole intermediate states are used.

The calculated W is also somewhat weaker than the empirical one, but it accounts for a large fraction (~71%) of the reaction cross section compared to empirical potentials when used in the Schrödinger equation. The total inelastic cross section, calculated directly with all natural parity intermediate states, accounts for ~60 mb which is less than 10% of the total reaction cross section.

The work presented here is closest to that of Vinh Mau and her collaborators,[5-7] and the theoretical formalism is based on her nuclear structure approach. Our principal improvements are the use of the optical Green's function for the intermediate-nucleon propagator, and the use of RPA wave functions which are more complete, having a larger particle-hole basis and including charge exchange channels. We would therefore expect to calculate a more absorptive potential. The fact that we do not is at least partly due to different projectile, target-nucleon interactions. The Reichstein-Tang[25] interaction used in Ref. 6 gives 50% more absorption than the Eikemeier-Hackenbroich interaction, which we use. However, it also gives a cross section for inelastic scattering to the first 3^- state which is about 50% too large when used with our transition densities.

The alternative method, the nuclear matter ap-

proach to the calculation of nuclear optical potentials, has had considerable success. Jeukenne *et al.*[2,3] use the local density approximation to obtain W in finite nuclei from that calculated in nuclear matter. Brieva and Rook,[4] on the other hand, make the local density approximation only on the effective two-body scattering operator t and then fold the resulting approximate t with the nuclear density. This approach should represent a substantial improvement over that of Refs. 2 and 3 in that the nuclear density, which changes rather rapidly in the nuclear surface, is treated more accurately.

However, the work in Ref. 2, 3, and 4 treats nuclear structure only in infinite matter. Both our results and those of Refs. 5 and 6 show large effects from nuclear collectivity. If particle-hole states are used, the resulting imaginary potential is both too weak and does not have the surface form expected on the basis of phenomenological imaginary optical potentials. The fact that imaginary optical potentials obtained in the nuclear matter[2,3] approach, which also uses sums over simple particle-hole states, do show a strong surface peaking represents a real discrepancy between the two theories. In the nuclear structure approach it is due to the collectivity, while in the nuclear matter approach it is simply an effect of the Pauli principle. In this connection it should be pointed out that the imaginary potential of Brieva and Rook[4] was both too weak for low-energy projectile and has essentially a volume form. These authors suspected and suggested that the inadequacy of a nuclear matter description of the nuclear spectrum at low energies might be the cause of their failure to obtain enough strength for W. This opinion is borne out by the nuclear-structure approach of Vinh Mau[5,6] and the work reported in this paper. The residual interaction lowers the strongly excited states in energy increasing the excitation strength at low energy and therefore also increasing W.

The nuclear matter approach has two additional features which will clearly result in erroneous estimates of the absorptive potential. First, since the Hamiltonian is translationally invariant, $T=0$, 1^- states are present in the spectrum. As the 1^- collective translational state is rather large, it can be expected to contribute considerably to the absorption, while in the finite-nucleus RPA spectrum such a spurious state is eliminated.

The second point is that in nuclear matter there is no energy gap, so even at low energies of a few MeV there will be open particle-hole states contributing to absorption. In the nuclear structure approach, these channels are eliminated by the gap, and only the low-lying collective states, which are pushed down in energy by the residual ph interaction, contribute to absorption.

There are a number of defects in the nuclear structure approach to the determination of the opical potential. The RPA does rather well in the calculation of transition probabilities, but the accuracy for the entire spectrum may not be very good. Different RPA calculations with different parameters may give different transition densities, even to particular states where the energies and $B(E\lambda)$ values are fitted. These differences would, of course, give rise to differences in the scattering. Furthermore, states of low multipolarity are more likely to be accurately described by an RPA calculation than those of higher multipolarity.

The weakest point is perhaps the use of an effective interaction instead of a t or G matrix calculated from realistic forces.[26] In our work and that of Ref. 6, the effective interaction used in the scattering and structure calculations was also different. With simple effective interactions it is not always possible to fit inelastic scattering cross sections for different multipole transitions simultaneously.

It should also be pointed out that in both the nuclear-matter and nuclear-structure approaches, the representation of the imaginary potential by a local equivalent is not expected to be very reliable. The nonlocality in some regions is rather large and the applicability of a local approximation is open to question.

Despite these difficulties and uncertainties we have, with no adjustment of parameters, been able to calculate an imaginary optical potential which is within about 34% of the phenomenological value and gives ~71% of the reaction cross section. The potential is surface peaked, as are typical phenomenological potentials, but the peak appears at a smaller radius. The shape in nuclear surface is, however, remarkably similar to the Ohio phenomenological potential,[24] which at 30 MeV has a volume form.

ACKNOWLEDGMENTS

We acknowledge important conversations concerning the theory of the microscopic optical potential with Prof. N. Vinh Mau, Dr. H. Ngo, and Dr. G. R. Satchler. We are appreciative of helpful conversations and support from Prof. A. Faessler. We are also grateful to Prof. J. Speth for supplying us with his RPA wave functions, for discussions concerning the nuclear structure, and for his continued interest and support. The work of V.A.M. was supported in part by the U.S.

Department of Energy under Contract No. EY-76-S-06-2227.

APPENDIX: DERIVATION OF EQ. (5)

In this appendix several approximations are made concerning the projectile, which allow us to treat it and the target nucleus on a different footing. Starting from the first term of Eq. (3), complete sets of eigenstates of H_0 are inserted to the right and to the left of each V factor between J and $J^\dagger$. These are $(N+1)$-particle, N-hole states, where N is arbitrary. The first approximation is that, when $J^\dagger$ operates to the right, it produces at least one particle state above the Fermi sea, which will be labeled q. This treatment neglects the refinements in the effects of the Pauli principle due to the fact that the operator to the right of $J^\dagger$ in the first term of Eq. (3) produces an exact ground state of the A-particle system when it operates on the vacuum state $|0\rangle$. Our approximation ignores the fact that some states below the Fermi energy are therefore empty and some states above it are occupied. Next we make the second-order approximation for the projectile. This consists in keeping only terms in the intermediate states in which the projectile quantum number q propagates without interaction. At each stage of interaction by V there is a factor of $N+1$ due to the $(N+1)$-like terms in which any intermediate particle state may be q. This factor $N+1$ is exactly compensated by a factor of $(N+1)^{-1}$ double-counting correction in the $(N+1)$-particle, N-hole state.

For example, consider such matrix elements in zeroth, first, and second orders in the V between J and $J^\dagger$. Aside from energy dominators they would have typical forms such as

$$\tfrac{1}{2}\langle 0|J|qmi\rangle\langle qmi|J^\dagger|0\rangle\,, \tag{A1a}$$

$$\tfrac{1}{4}\langle 0|J|pmi\rangle\langle pmi|V|nrj\rangle\langle nrj|J^\dagger|0\rangle\,, \tag{A1b}$$

$$\tfrac{1}{4\cdot 3!}\langle 0|J|pmi\rangle\langle pmi|V|rstil\rangle \times\langle rstil|V|nvj\rangle\langle nvj|J^\dagger|0\rangle. \tag{A1c}$$

In Eq. (A1a) it is arbitrary which particle quantum number is designated as belonging to the projectile but we take it to be q. The factor of $\frac{1}{2}$ is introduced to compensate for the fact that each of q and m is allowed to take on all particle quantum numbers. Likewise the factor $\frac{1}{4}$ in Eq. (A1b) compensates for double counting both between p,m, and n,r particle quantum numbers, and the extra factor $(3!)^{-1}$ in Eq. (A1c) compensates for double counting among r, s, t. In Eq. (A1b) one of the particle quantum numbers p or m will not be involved in the interaction and will be equal to one of n or r. Whichever one it is, we label it as q and designate it as the projectile quantum number. Since there are 2×2 possibilities for q, we get a factor of 4 times an amplitude with the sequence of particle quantum numbers qm, qn appearing in the intermediate states. In Eq. (A1c) there are $2\times 3\times 2$ choices for a fixed quantum number, which is again labeled as q, leaving a factor of $\frac{1}{2}$ and the sequence of particle quantum numbers $qm\ qst\ qv$. The remaining factor of $\frac{1}{2}$ compensates for the double counting between the other intermediate particle quantum numbers st; therefore, only in the lowest order, Eq. (A1a), does the double counting factor involving the projectile remain. We now add and subtract a term identical to Eq. (A1a); this subtracted term is the double counting correction.

The quantum number q is produced by $J^\dagger$ and destroyed by J, serving as a spectator during the r interactions of the intermediate V. The energy denominator is allowed to operate on these intermediate states to the extent that the q term in the zero-order Hamiltonian

$$H_0=\sum_k \epsilon_k a_k^\dagger a_k \tag{A2}$$

is evaluated, producing a term ϵ_q in each energy denominator. The only matrix elements to be evaluated involving q are the creation of q by $J^\dagger(k)$ and its destruction by $J(k')$; both of these produce the same type of Hermitian one-body operator, for example,

$$[J(k'),a_q^\dagger]=\sum_{\beta\gamma} a_\beta^\dagger\langle k'\beta|V|q\delta\rangle_A a_\delta \equiv J(k',q)\,, \tag{A3}$$

where

$$\langle k'\beta|V|q\delta\rangle_A=\langle k'\beta|V|q\delta\rangle-\langle k'\beta|V|\delta q\rangle\,. \tag{A4}$$

The second term of Eq. (3) does not contribute to the imaginary potential because the energy denominators are always nonzero. With the approximations described above we obtain the result

$$\mathrm{Im}v(\vec{k}',k)=\mathrm{Im}\sum_{q>f}\left[\sum_{prs}\left\langle 0\left|\left(V\frac{1}{E_0-H_0}\right)^p J(\vec{k}',\vec{q})\frac{1}{E-\epsilon_q-H_0+i\eta}\left(V\frac{1}{E-\epsilon_q-H_0+i\eta}\right)^r J(q,k)\left(\frac{1}{E_0-H_0}V\right)^s\right|0\right\rangle -\tfrac{1}{2}\langle 0|J(k',q)\frac{1}{E-\epsilon_q-H_0+i\eta}J(q,k)|0\rangle\right], \tag{A5}$$

where H_0 and V operate now only on the target nuclear state. The subscript LC has been dropped because,

with the approximations which have been made, no unlinked or reducible graphs remain.

The Pauli principle is again violated in Eq. (A5) by intermediate states of the A particle system between $J(k',q)$ and $J(q,k)$ in which a particle occupies the state q. Since the projectile degree of freedom has now been removed, the operator between $J(k',q)$ and $J(k,q)$ operates now only on the A particle system. It can then be summed to give

$$\sum_r \frac{1}{E-\epsilon_q-H_0+i\eta}\left(V\frac{1}{E-\epsilon_q-H_0+i\epsilon}\right)^r=\frac{1}{E-\epsilon_q-H+i\epsilon}\,, \tag{A6}$$

but the H operates only on intermediate target states. Equations (A5) and (2) may now be written as

$$W(k',k)=\mathrm{Im}\sum_{N\neq 0,q>f}\left[\langle\Psi_0|J(k',q)|\Psi_N\rangle\frac{1}{E-\epsilon_q-E_N+i\eta}\langle\Psi_N|J(q,k)|\Psi_0\rangle\right.$$
$$\left.-\tfrac{1}{2}\langle\varphi_0|J(k',q)|\varphi_N\rangle\frac{1}{E-\epsilon_q-E_N^{(0)}+i\eta}\langle\varphi_N|J(q,k)|\varphi_0\rangle\right], \tag{A7}$$

where $W(k',k)=\mathrm{Im}v(k',k)$ and Ψ_N and Ψ_0 are, in principle, exact eigenstates, while φ_N and φ_0 are eigenstates of H_0 for the A-particle target system. It is perhaps worth mentioning that the last term of Eq. (A7) can be written as a sum of four terms, which, when all the matrix elements are evaluated, may be designated as DD, DE, ED, and EE, where D stands for *direct* and E for *exchange*. The DD term is topologically identical to the EE term, and DE, ED to each other. We could have written the last term of Eq. (A7) as a sum without the $\frac{1}{2}$ of just the ED and EE terms. Subtraction of this double counting term then eliminates from the lowest-order contributions of the first term of Eq. (A6) topologically identical graphs, thereby satisfying the rule[15] that only topologically distinct graphs are included in the calculation of the mass or self-energy operator.

In actual calculations, the single-particle representations for target and projectile are usually not the same. The RPA calculations for the target use discretized particle states for the continuum, and the scattering calculation uses an optical Green's function to describe the sum over intermediate states. If the q and m sums are complete, this is not a deficiency in the calculation. The intermediate sum over 2-particle–1-hole states nmi in an equal basis can be written

$$\tfrac{1}{2}\sum_{mni}|nmi\rangle\langle nmi|\,, \tag{A8}$$

where the factor of $\frac{1}{2}$ corrects the double counting, so both m and n are allowed to take on all particle quantum numbers.

We may now transform to a different complete single-particle basis q for the projectile

$$|n\rangle=\sum_q C_{nq}|q\rangle\,. \tag{A9}$$

Substitution of Eq. (A9) in Eq. (A8) and summation over n then gives simply

$$\tfrac{1}{2}\sum_{qmi}|qmi\rangle\langle qmi|\,. \tag{A10}$$

We assume that our RPA particle-hole basis for the intermediate states is sufficiently complete to include all significant particle-hole strength and therefore truncate m, while the q sum is allowed to remain complete. With this truncation the correction factor of $\frac{1}{2}$ must be included for all the second-order matrix elements, and all four terms DD, DE, ED, and EE are kept as in the second term of Eq. (5).

An additional important point is that if the neutrons and protons are treated as identical the charge exchange intermediate states ${}^{A}_{Z}X_N(n,p)^{A}_{Z-1}Y(p,n)^{A}_{Z}X_N$ must be retained as well as inelastic states. If they are not kept, there is no double counting when q is a neutron and mi is a proton particle-hole pair.

*Present address: Department of Physics, State University of New York at Stony Brook, Stony Brook, N. Y. 11794.

[1]J. S. Bell and E. J. Squires, Phys. Rev. Lett. 3, 96 (1959); J. S. Bell, *Lectures on the Many-Body Problem*, edited by E. R. Caianello (Academic, New York, 1962).

[2]J. P. Jeukenne, A. Lejeune, and C. Mahaux, Phys. Rep. 25, 83 (1976).

[3]C. Mahaux, *Microscopic Optical Potentials*, *Lecture Notes in Physics*, edited by H. V. Geramb (Springer, Berlin, 1979), p. 1.

[4]F. Brieva and J. R. Rook, Nucl. Phys. A291, 299 (1977); A291, 317 (1977); A307, 493 (1978).

[5]N. Vinh Mau and A. Bouyssy, Nucl. Phys. A257, 189 (1976).
[6]N. Vinh Mau, *Microscopic Optical Potentials, Lecture Notes in Physics*, edited by H. V. Geramb (Springer, Berlin, 1979), p. 40.
[7]V. Bernard and N. van Giai, Nucl. Phys. A327, 397 (1979).
[8]V. Gillet and E. A. Sanderson, Nucl. Phys. 54, 472 (1964); A91, 292 (1967).
[9]C. L. Rao, M. Reeves III, and G. R. Satchler, Nucl. Phys. A207, 182 (1973).
[10]H. Feshbach, Ann. Phys. (N.Y.) 19, 287 (1962).
[11]P. W. Coulter and G. R. Satchler, Nucl. Phys. A293, 269 (1977).
[12]H. Eikemeier and H. H. Hackenbroich, Nucl. Phys. A169, 407 (1971).
[13]S. Krewald and J. Speth, Phys. Lett. 74B, 295 (1974).
[14]F. G. Perey and D. S. Saxon, Phys. Lett. 10, 107 (1964).
[15]A. L. Fetter and J. D. Walecka, *Quantum Theory of Many-Particle Systems* (McGraw-Hill, New York, 1976).
[16]F. Villars, in *Fundamentals of Nuclear Theory*, edited by A. de Shalit and C. Villi (IAEA, Vienna, 1967).
[17]J. Wambach, F. Osterfeld, J. Speth, and V. A. Madsen, Nucl. Phys. A324, 77 (1979).
[18]V. A. Madsen, in *Nuclear Spectroscopy and Reactions* (Academic, New York, 1975).
[19]H. Horie and K. Sasaki, Prog. Theor. Phys. 25, 475 (1961).
[20]G. E. Brown, *Unified Theory of Nuclear Models* (North-Holland, Amsterdam, 1964).
[21]A. Lev, W. P. Beres, and M. Davideenum, Phys. Rev. C 9, 2416 (1974).
[22]F. D. Becchetti and G. W. Greenlees, Phys. Rev. 182, 1190 (1969).
[23]A. M. Green, Phys. Lett. 24B, 384 (1967).
[24]J. Rapaport, V. Kulkarni, and R. W. Finlay, Nucl. Phys. A330, 15 (1979); J. Rapaport, J. D. Carlson, D. Bainum, T. S. Cheema, and R. W. Finlay, *ibid.* A286, 232 (1977).
[25]I. Reichstein and Y. C. Tang, Nucl. Phys. A139, 144 (1969).
[26]V. A. Madsen, F. Osterfeld, and J. Wambach, in *Microscopic Optical Potentials, Lecture Notes in Physics*, edited by H. V. Geramb (Springer, Berlin, 1979), p. 151.